Crosstalk error correction through dynamical decoupling of single-qubit gates in capacitively coupled singlet-triplet semiconductor spin qubits

Donovan Buterakos, Robert E. Throckmorton, and S. Das Sarma
Condensed Matter Theory Center and Joint Quantum Institute, Department of Physics, University of Maryland, College Park, Maryland 20742-4111, USA

(Received 10 November 2017; published 29 January 2018)

In addition to magnetic field and electric charge noise adversely affecting spin-qubit operations, performing single-qubit gates on one of multiple coupled singlet-triplet qubits presents a new challenge: crosstalk, which is inevitable (and must be minimized) in any multiqubit quantum computing architecture. We develop a set of dynamically corrected pulse sequences that are designed to cancel the effects of both types of noise (i.e., field and charge) as well as crosstalk to leading order, and provide parameters for these corrected sequences for all 24 of the single-qubit Clifford gates. We then provide an estimate of the error as a function of the noise and capacitive coupling to compare the fidelity of our corrected gates to their uncorrected versions. Dynamical error correction protocols presented in this work are important for the next generation of singlet-triplet qubit devices where coupling among many qubits will become relevant.

DOI: 10.1103/PhysRevB.97.045431

I. INTRODUCTION

Correcting for error in operations on qubits is of utmost importance to building a working quantum computer. The fact that quantum error correction is possible is what started the whole world-wide effort in trying to build a practical quantum computer. Operations on qubits require very high precision and accuracy; in fact, a fidelity of at least 99% is required to implement error correction using surface codes [1]. Other error correction techniques require an even higher fidelity of 99.99%. Several different platforms for realizing qubits exist, but our focus in this work will be on electronic spins in semiconductor quantum dots. Several different types of semiconductor quantum dot electron spin qubits exist, such as the single-spin exchange qubit [2–9], the singlet-triplet two-electron double-dot qubit [10–19], the exchange-only three-electron triple-dot qubit [20–24], and the "hybrid" three-electron double-dot qubit [25–27]. The semiconductor spin-qubit platform has the advantages of being compatible with the existing semiconductor electronics industry as well as the ability to perform gates more quickly (using fast electrical pulses) than other platforms, such as superconducting and ion trap qubits. Other perceived advantages of semiconductor spin qubits include the scalability inherent in semiconductors and the relatively long spin relaxation times in solids. However, noise-induced error has been a formidable challenge adversely affecting experimental progress in spin qubits. Fortunately, considerable progress has been achieved recently, with single-qubit gate fidelities of 99% and two-qubit gate fidelities of 90% having been reported in singlet-triplet double-dot qubits [28]. Several methods for reducing error have been developed for these platforms. Methods such as isotopic purification in Si and polarization of nuclei in GaAs reduce noise at the materials level simply by eliminating the sources of field noise. Other methods instead combat the effects of noise through pulse control techniques such as dynamical decoupling, Bayesian estimation of parameters, and designing dynamically corrected pulse sequences that partially cancel the effects of noise [17,29–33]. The goal is to sufficiently reduce both one- and two-qubit gate errors in the physical qubits so that surface code architectures become feasible, eventually leading to quantum error corrections producing logical qubits.

In spite of enormous progress over the last 5–10 years, the experimental situation in semiconductor spin qubits is still somewhat discouraging compared with superconducting and ion trap qubits since reasonable two-qubit gate operations have only been demonstrated in singlet-triplet qubits in GaAs with the fidelity improving from [15] 70% to [28] 90% over the 2012–2017 five-year period. Although single-qubit fidelity approaching or even exceeding 99% has been reported for both single spin and singlet-triplet qubits, these experiments are not carried out in multiqubit platforms and, therefore, one does not know the limiting single-qubit fidelity in circuits where multiple qubits are being operated. Given that the most advanced gate operations by far have happened so far only in the singlet-triplet spin qubits, our focus in this work is entirely on this system. The specific issue we address is the mitigation of crosstalk errors where the quantum computing platform consists of many singlet-triplet qubits with single-qubit gate operations going on simultaneously in many of them, as would eventually be necessary for any meaningful quantum information processing task.

There has been considerable work on error correction techniques in semiconductor quantum dot systems. For the single-electron exchange qubit, NMR-inspired decoupling techniques such as the Carr-Purcell-Meiboom-Gill (CPMG) technique, a generalization of the Hahn echo technique [34–36], exist. Unfortunately, these techniques cannot be applied to singlet-triplet qubits, which are the focus of this work. These generalized spin-echo-type protocols for restoring quantum coherence require one to be able to apply, for example, a π rotation pulse and then later apply a $-\pi$ rotation pulse about the same axis, which cannot be done in existing experimental singlet-triplet

systems. To see why, we consider the effective Hamiltonian for a singlet-triplet qubit within the logical subspace, which is

$$H = J(t)Z + hX, \tag{1}$$

where $J(t)$ is the exchange coupling, h is the magnetic field difference between the two qubits, and X and Z are the Pauli matrices. The magnetic field difference is realized using a micromagnet or by polarizing the nuclei (if possible). This difference may in principle also be realized by electrically tuning the effective g factors in the quantum dots [37–39], but this technique has not been used in any singlet-triplet qubit experiment to date. It is very difficult to control this field difference quickly in the actual experiments, and thus it is held constant. This means that all control is achieved by electrically tuning the exchange coupling, either by tilting the dot potential or by changing the height of the potential barrier between them so that the wave-function overlap is modified. Furthermore, at least in the presence of just two electrons, it is very difficult to make the exchange coupling negative. We should note, however, that it can be made negative in a sufficiently strong magnetic field or in the presence of more than two electrons [40–42], though the presence of these additional electrons enlarges the total Hilbert space of the system, creating a new set of challenges such as leakage errors. All of this means that we cannot apply the time-reversed version of a given pulse or pulse sequence in a singlet-triplet qubit. We must therefore seek other methods for error correction through dynamical decoupling.

There have been several papers proposing dynamically corrected pulse sequences for performing single-qubit singlet-triplet gates. Three papers have been written using the SUPCODE technique, one for the case in which only (electrical) charge noise is present [43] and two others in which (magnetic) field noise is also included [44,45]. This method, which we will be employing a generalization of in this work, consists of inserting an uncorrected "identity" operation into the pulse sequence for a given gate that is arranged in such a way as to cancel the noise-induced error to leading order. These works consider sequences of square pulses; another work [46] considers the case with only field noise and proposes smooth pulses that cancel noise-induced error to arbitrary orders. In relation to two-qubit operations, the problem of the dynamics of two coupled singlet-triplet qubits under the influence of noise has been investigated [47], and a recent paper discusses the fidelity for realizing a maximally entangled state from a tensor-product state [48]. Dynamical error correction has also been investigated for controlled-NOT (CNOT) gates, first to a limited extent in Ref. [44] and then in more detail in Ref. [49]. While correcting for noise-induced error is important, it is not the only issue that needs to be addressed in the context of practical quantum information processing. At least one two-qubit entangling operation, along with the ability to perform arbitrary single-qubit gates, is necessary to achieve universal quantum computation. Thus, one must consider also the coupling among the singlet-triplet qubits.

Unfortunately, the couplings between qubits required to perform two-qubit operations also adversely affect single-qubit operations via crosstalk. However, as discussed later, the strength of the capacitive coupling is proportional to the value of the exchange couplings J for each qubit, so one could set J for the neighboring qubit to zero while performing the single-qubit gate to counter this problem. Unfortunately, this poses two problems. First, there are experimental limitations in setting J to exactly zero, and thus some small crosstalk would still persist. Second, a dynamical pulse sequence is required even for qubits on which no gates are performed to maintain coherence. Therefore, in order to be compatible with a large-scale architecture, it is necessary to address the system as a whole, which is in fact the subject of this work. Our dynamical decoupling sequence for correcting crosstalk errors (along with field and charge noise) is not an essential ingredient for the currently ongoing experiments where one has at best only two qubits coupled with each other. But, this is of course a very primitive state of affairs as far as quantum computing goes. Eventually, the platform must consist of many coupled qubits with substantial crosstalk among them. Our work will become an important ingredient when both single- and multiqubit gate operations are being carried out in quantum computing platforms with many coupled singlet-triplet qubits. Our work is also relevant to a system containing only two singlet-triplet qubits where the exchange coupling within the qubit cannot simply be tuned to zero while turning on the two-qubit capacitive coupling.

We will be considering here two capacitively coupled singlet-triplet qubits. This form of coupling, which is used extensively for interqubit coupling in singlet-triplet qubits [15,28], is simpler to treat than a Heisenberg exchange coupling since capacitive coupling, as we will see, cannot cause leakage out of the logical subspace. We also assume that the field and charge noise in our system is quasistatic. As noted earlier, our approach to dynamical error correction is a generalization of the SUPCODE approach of Refs. [44,45] and, like this approach, the overall idea is to insert an uncorrected "identity" operation into the pulse sequence for a given gate that is arranged in such a way as to cancel both noise- and crosstalk-induced error to leading order. We begin by deriving expressions giving the noise- and crosstalk-induced error to leading order for a single pulse (i.e., all Hamiltonian parameters held constant). From this, we show how to derive the error for a general, multipulse, sequence. Our error correction procedure consists of first applying our "naïve" pulse sequence for a given gate to the qubits, and then following that with an uncorrected "identity" with its parameters arranged in such a way as to cancel both noise- and crosstalk-induced errors. This "identity" consists of a set of "blocks" of pulse sequences such that one qubit is subject to a single pulse and the other is subject to two pulses with a combined duration equal to that of the single pulse; we adopt such a form for mathematical simplicity. We then determine the parameters needed to make the sum of the errors from the "naïve" sequence and the "identity" zero. We present the parameters that we extract from this procedure for all 24 Clifford gates and present an example, a rotation by π about the $\hat{\hat{x}} + \hat{\hat{y}}$ axis. Overall, the resulting pulse sequences consist of more "blocks" (up to nine) than those used to correct only noise-induced error for a single qubit in isolation. The presence of crosstalk also forces us to propose sequences that never set the exchange couplings to their maximum experimentally possible values. This is because the capacitive coupling strength is proportional to the exchange couplings, and thus large exchange couplings will result in more crosstalk. We then, as an important check,

demonstrate that these proposed error-corrected sequences do, in fact, cancel noise- and crosstalk-induced errors to leading order.

The rest of the paper is organized as follows. In Sec. II, we present our model and derive the formulas for the noise- and crosstalk-induced error to first order. Section III details our dynamical error correction scheme, presents the mathematical form of the corrected pulse sequences in terms of a set of numerical parameters, and demonstrates that our correction scheme does in fact cancel the leading-order noise- and crosstalk-induced error. We give our conclusions in Sec. IV, and provide the specific numerical values of the parameters for the dynamically corrected pulse sequences implementing the Clifford gates in Appendix A. We also provide in Appendix B the dynamical decoupling pulse sequences for a different model of the interqubit coupling, where the coupling is independent of the intraqubit exchange energy.

II. MODEL

A. Hamiltonian

A singlet-triplet (ST) qubit consists of a pair of quantum dot spins coupled by the exchange interaction with a computational basis given by $|0\rangle = \frac{1}{\sqrt{2}}(|\uparrow\downarrow\rangle + |\downarrow\uparrow\rangle)$ and $|1\rangle = \frac{1}{\sqrt{2}}(|\uparrow\downarrow\rangle - |\downarrow\uparrow\rangle)$. Single-qubit control is obtained by applying a magnetic field gradient h across the two quantum dots and by varying the strength of the exchange interaction J, yielding the single-qubit Hamiltonian $H = hX + JZ$, where X and Z are Pauli matrices in the logical basis. However, due to physical limitations of the system, these parameters incur several constraints. First, the time scale on which the magnetic field gradient can be varied is much longer than the time needed to vary the exchange coupling, so, in practice, h is held constant. Second, the strength of the exchange interaction J must be positive and, in general, bounded between some values $j_{\min}$ and $j_{\max}$. Thus, axes of rotation are limited to the first quadrant of the xz plane.

We consider a system of two such ST qubits with a large enough potential barrier that there is no exchange interaction between the two separate qubits, but close enough that a capacitive interqubit coupling of strength J_{12} is present between them. This coupling arises from the difference in charge distributions between the two quantum dots of a ST qubit. When a ST qubit is in the singlet state $|1\rangle$, the charge distribution between the two quantum dots is asymmetric, producing a dipole moment. If instead the qubit is in the triplet state $|0\rangle$, the charge distribution is symmetric, so no dipole moment is present. The Hamiltonian thus includes a dipole-dipole interaction which contributes only when both qubits are in the singlet state [15]. The strength of this coupling term is proportional to both J_1 and J_2, and we will set the proportionality constant ε. Thus, for a system of two capacitively coupled singlet-triplet qubits we have the following Hamiltonian:

$$H = h_1X_1 + h_2X_2 + J_1Z_1 + J_2Z_2 + \varepsilon J_1J_2(Z_1 - 1)(Z_2 - 1). \tag{2}$$

While the capacitive coupling term of the above Hamiltonian has often been quoted as an experimentally established fact, and not derived from any model, it is possible to put it on a more rigorous footing as follows. Let us consider the Hubbard model Hamiltonian for the double-dot system considered in Ref. [50] (Eq. (A3), minus the H_J terms, which are only present when there are more than two electrons in the double-dot system [40,41]):

$$H = H_e + H_t + H_U, \tag{3}$$

with

$$H_e = \sum_{k=1}^{2} \epsilon_k n_k, \tag{4}$$

$$H_t = t \sum_{\sigma=\uparrow,\downarrow} c_{1\sigma}^{\dagger} c_{2\sigma} + \text{H.c.}, \tag{5}$$

$$H_U = U \sum_{k=1}^{2} n_{k\uparrow} n_{k\downarrow} + U' n_1 n_2. \tag{6}$$

The $c_{k\sigma}$ operators annihilate an electron in dot k with spin σ, $n_{k\sigma} = c_{k\sigma}^{\dagger} c_{k\sigma}$ is the number of electrons of spin σ in dot k, and $n_k = \sum_\sigma n_{k\sigma}$. Throughout, we will assume that $U, U' \gg t$. We can write the dipole moment as $\vec{d} = \frac{1}{2} e\vec{a}(n_2 - n_1)$, with e the electron charge and $\vec{a}$ the vector pointing from the first quantum dot to the second. If we let $\epsilon_1 = \epsilon_0 - \frac{1}{2}\Delta\epsilon$ and $\epsilon_2 = \epsilon_0 + \frac{1}{2}\Delta\epsilon$, then we may write

$$\vec{d} = e\vec{a}\frac{\partial H}{\partial \Delta\epsilon}. \tag{7}$$

By the Feynman-Hellmann theorem, we find that the expectation value of this dipole moment operator is just

$$\langle \vec{d} \rangle = e\vec{a}\frac{\partial E}{\partial \Delta\epsilon}, \tag{8}$$

where E is the (expectation value of the) energy of the system. The derivative of this energy will be zero in the triplet state since the Pauli exclusion principle would forbid both electrons from occupying the same dot, even if $\epsilon_1 \neq \epsilon_2$. Therefore, only the singlet state will have a dipole moment. However, in this case, the energy difference between the singlet and triplet states just gives the exchange coupling J, so that the expectation value of the dipole moment in the singlet state is just

$$\langle \vec{d} \rangle = e\vec{a}\frac{\partial J}{\partial \Delta\epsilon}, \tag{9}$$

and is zero in the triplet state.

To establish that $|\langle \vec{d} \rangle| \propto J$, we now use Eq. (A14) of Ref. [50] (again, minus contributions from the H_J terms):

$$J = \frac{4t^2}{U - U' - |\Delta\epsilon|}. \tag{10}$$

For $|\Delta\epsilon| \ll U - U'$,

$$\frac{\partial J}{\partial \Delta\epsilon} \approx \frac{4t^2}{(U - U')^2}\text{sgn}(\Delta\epsilon) = \frac{J}{U - U'}\text{sgn}(\Delta\epsilon) \tag{11}$$

and, therefore,

$$\langle \vec{d} \rangle \approx \frac{eJ}{U - U'}\text{sgn}(\Delta\epsilon)\vec{a}. \tag{12}$$

There will be corrections to this formula, but these will be small, as they are proportional to powers of $\frac{|\Delta\epsilon|}{U - U'}$. Experimental data on noise in the system imply that $\frac{\partial J}{\partial \epsilon} \propto J$, so it seems

that, at least in experimental systems, this approximation works very well qualitatively.

Finally, to obtain the interaction term for two double-dot systems, we may approximate it using the classical dipole-dipole interaction potential

$$U_{dd} = \frac{3(\vec{d}_1 \cdot \vec{r})(\vec{d}_2 \cdot \vec{r}) - \vec{d}_1 \cdot \vec{d}_2 r^2}{r^5}, \tag{13}$$

where $\vec{r}$ is the vector pointing from one dipole to the other. We can already see from our previous result simply by substituting in the expectation values of the dipole moments of the double dots that this will be proportional to $J_1 J_2$ when both double dots are in the singlet state, with the proportionality factor being determined by the relative position and orientation of the double dots, and zero otherwise, thus establishing the capacitive coupling term given in Eq. (2).

We should note that arriving at these expressions required a number of simplifying approximations; a more detailed analysis of this problem, starting from a microscopic model of the full four-dot system, would be required to give a fully rigorous justification of this form. While such a calculation would be of great interest, it is beyond the scope of this work, where we stick to Eq. (2) as describing the interqubit coupling Hamiltonian as used extensively in the theoretical literature on singlet-triplet qubits.

B. Expansion of evolution operator

In practice [15], εJ_i is found to be on the order of $\frac{1}{300}$, so we choose to approach this problem by performing a power-series expansion in ε. This allows us to consider a simplified Ising interaction term of the form $\varepsilon J_1 J_2 Z_1 Z_2$ since the terms $-\varepsilon J_1 J_2 Z_i$ can be absorbed into the $J_i Z_i$ terms without affecting the result to first order in ε [see Eq. (19)]. For convenience, we introduce the shorthand $a_i = \sqrt{h_i^2 + J_i^2}$, and perform the expansion in the rotated frame given by

$$\begin{aligned} X_i' &= (h_i X_i + J_i Z_i)/a_i, \\ Y_i' &= Y_i, \\ Z_i' &= (-J_i X_i + h_i Z_i)/a_i. \end{aligned} \tag{14}$$

This frame preserves the standard Pauli commutation relations for X_i', Y_i', and Z_i'. Using this notation, the Hamiltonian can be expressed as

$$H = a_1 X_1' + a_2 X_2' + \frac{\varepsilon J_1 J_2}{a_1 a_2}(J_1 X_1' + h_1 Z_1')(J_2 X_2' + h_2 Z_2'). \tag{15}$$

Using the identity for the exponential of a sum of operators,

$$e^{-it(A+\varepsilon B)} = e^{-itA}\left[1 + (-it)\varepsilon B - \frac{(-it)^2}{2!}\varepsilon[A,B] + \frac{(-it)^3}{3!}\varepsilon[A,[A,B]] - \cdots\right] + O(\varepsilon^2), \tag{16}$$

with $A = a_1 X_1' + a_2 X_2'$ and $B = (J_1 X_1' + h_1 Z_1')(J_2 X_2' + h_2 Z_2')$, we can evaluate the commutators on the right side and resum the series, yielding a closed-form expression for the evolution operator e^{-itH} to first order in ε. The result we obtain is

$$e^{-itH} = e^{-it(a_1 X_1' + a_2 X_2')}\left(1 - i\sum_{i'j'} \Delta^{\text{cap}}_{i'j'} \sigma_{i'} \otimes \sigma_{j'}\right), \tag{17}$$

where $\sigma_{i'}$ and $\sigma_{j'}$ are the rotated Pauli matrices defined by Eq. (14), and the $\Delta^{\text{cap}}_{i'j'}$ are given by

$$\begin{aligned} \Delta^{\text{cap}}_{X_1'X_2'} &= \varepsilon \frac{J_1^2 J_2^2}{a_1 a_2} t, \\ \Delta^{\text{cap}}_{Y_1'Y_2'} &= \varepsilon \frac{J_1 J_2 h_1 h_2}{2 a_1 a_2}\{-t\,\text{sinc}\,[2(a_1 + a_2)t] \\ &\quad + t\,\text{sinc}\,[2(a_1 - a_2)t]\}, \\ \Delta^{\text{cap}}_{Z_1'Z_2'} &= \varepsilon \frac{J_1 J_2 h_1 h_2}{2 a_1 a_2}\{t\,\text{sinc}\,[2(a_1 + a_2)t] \\ &\quad + t\,\text{sinc}\,[2(a_1 - a_2)t]\}, \\ \Delta^{\text{cap}}_{X_1'Y_2'} &= \varepsilon \frac{J_1^2 J_2 h_2}{a_1} t^2\,\text{sinc}^2\,(a_2 t), \\ \Delta^{\text{cap}}_{X_1'Z_2'} &= \varepsilon \frac{J_1^2 J_2 h_2}{a_1 a_2} t\,\text{sinc}\,(2a_2 t), \\ \Delta^{\text{cap}}_{Y_1'Z_2'} &= \varepsilon \frac{J_1 J_2 h_1 h_2}{2 a_1 a_2}\{(a_1 + a_2)t^2\,\text{sinc}^2\,[(a_1 + a_2)t] \\ &\quad + (a_1 - a_2)t^2\,\text{sinc}^2\,[(a_1 - a_2)t]\}. \end{aligned} \tag{18}$$

The terms $\Delta^{\text{cap}}_{Y_1'X_2'}$, $\Delta^{\text{cap}}_{Z_1'X_2'}$, and $\Delta^{\text{cap}}_{Z_1'Y_2'}$ can be obtained by swapping the subscripts 1 and 2. We write the error in terms of $\text{sinc}\,x = \lim_{x' \to x} \frac{\sin x'}{x'}$ so that the error will be well defined when $a_1 - a_2 = 0$. Since the rotated Pauli matrices X_i', Y_i', and Z_i' depend on the J_i, which changes at different points in time, it is necessary to transform Eq. (18) back to the standard basis using Eq. (14). The result of this substitution, which involves considerable algebra and is not particularly illuminating, is not shown for the sake of space.

We now consider the addition of charge and field noise on each qubit. If the noise varies slowly compared to the total gate implementation time (i.e., quasistatic noise, often a very reasonable approximation for semiconductor spin qubits), we can treat the noise as small, unknown shifts to the values h_i and J_i. Thus, the complete Hamiltonian is

$$\begin{aligned} H &= (h_1 + dh_1)X_1 + (h_2 + dh_2)X_2 \\ &\quad + (J_1 + dJ_1 - \varepsilon J_1 J_2)Z_1 + (J_2 + dJ_2 - \varepsilon J_1 J_2)Z_2 \\ &\quad + \varepsilon J_1 J_2 Z_1 Z_2. \end{aligned} \tag{19}$$

We choose to work in the quasistatic noise limit, where these shifts do not directly depend on time. Thus, we will treat dh_i as constant for the entire pulse sequence, and dJ_i as a function solely of J_i. This is generally taken to be a linear relationship due to the underlying dependence of J_i on the quantum dot detuning [44]; however, since our method is a generalization of SUPCODE, it inherits SUPCODE's robustness in handling different dependencies of dJ_i on J_i, as long as the forms of such dependencies are known and sufficiently well behaved. In this work, we assume $dJ_i = \alpha_i J_i$ for some small constant parameter α_i. Expansions similar to the one above have already been performed [51] for the case of noise on a single qubit, and the presence of a second qubit will not affect

the first order terms of these expansions. Additional terms of order εdh_i or εdJ_i will appear, but since both the strength of the coupling and the magnitude of the error are small, such terms are second order and can be ignored. Combining this with the expansion of the Ising term done above, we obtain

$$e^{-itH} = e^{-it(h_1X_1+J_1Z_1)}e^{-it(h_2X_2+J_2Z_2)} \times\Bigg[1 - i\sum_i \Delta_i^{q1}\sigma_i\otimes 1 - i\sum_i \Delta_i^{q2} 1\otimes\sigma_i - i\sum_{ij}\Delta_{ij}^{cap}\sigma_i\otimes\sigma_j\Bigg], \tag{20}$$

where the Δ_{ij}^{cap} are given by Eq. (18) rotated into the standard basis as discussed above and the Δ_i^{qn} are given by

$$\begin{aligned}
\Delta_x^{qn} &= \frac{2h_n^2a_nt + J_n^2\sin 2a_nt}{2a_n^3}dh_n \\
&\quad + \frac{h_nJ_n(2a_nt - \sin 2a_nt)}{2a_n^3}(dJ_n - \varepsilon J_1J_2), \\
\Delta_y^{qn} &= \frac{J_n(\cos 2a_nt - 1)}{2a_n^2}dh_n \\
&\quad + \frac{h_n(1 - \cos 2a_nt)}{2a_n^2}(dJ_n - \varepsilon J_1J_2), \\
\Delta_z^{qn} &= \frac{h_nJ_n(2a_nt - \sin 2a_nt)}{2a_n^3}dh_n \\
&\quad + \frac{2J_n^2a_nt + h_n^2\sin 2a_nt}{2a_n^3}(dJ_n - \varepsilon J_1J_2).
\end{aligned} \tag{21}$$

There are 27 independent error terms: the 6 components Δ_i^{qn} each have three terms corresponding to dh_n, dJ_n, and ε, plus the 9 components Δ_{ij}^{cap} which have only a single term each.

III. ERROR CORRECTION

In order to develop dynamically corrected rotation sequences, it is necessary to examine in general how errors from consecutive rotations are combined. To that end, let R represent an ideal rotation (with no error or crosstalk) for given values of J_1, J_2, and t; U the corresponding uncorrected rotation; and Δ_R the first-order error in the rotation, so that $U = R(1 + \Delta_R)$, which has the same form as Eq. (20). We also let $M = R_1R_2\ldots R_m$ be a sequence of m ideal rotations and Δ_M the total error of the sequence of corresponding uncorrected rotations, so that $M(1 + \Delta_M) = U_1U_2\ldots U_m$. We can then increase the sequence by one additional rotation using the following equation, which holds to first order in Δ_M and Δ_R:

$$M(1 + \Delta_M)U = MR(1 + R^\dagger\Delta_MR + \Delta_R). \tag{22}$$

Recursively applying this equation allows the error of an arbitrary number of gates to be combined. The result is that the total error is a modified sum of the individual errors Δ_R, where each term in the sum is rotated by the inverse of all rotations which occur before (to the right of) R as shown below:

$$\prod_{i=1}^m U_i = \left(\prod_{i=1}^m R_i\right)\left[1 + \sum_{i=1}^m\left(\prod_{j=m}^{i+1} R_j^\dagger\right)\Delta_{R_i}\left(\prod_{j=i+1}^m R_j\right)\right]. \tag{23}$$

In order to perform a corrected gate, we follow a strategy similar to the one proposed in Ref. [44], in which a simple set of uncorrected rotations that implements the desired gate is performed, followed by a longer uncorrected identity operation which is designed to exactly cancel the first-order error in the initial rotations. The error term of the initial rotation, which we will call Δ_{rot}, can be directly calculated from Eqs. (18) and (21). The problem now becomes finding an uncorrected identity with an error term $\Delta_{idt} = -\Delta_{rot}$, i.e., an uncorrected identity with a total error that exactly cancels the error in the initial rotation. The simplest way to do this is by introducing a family of identity operations described by a set of free parameters, writing Δ_{idt} in terms of these parameters, and then numerically solving the equations $\Delta_{idt} + \Delta_{rot} = 0$. Since there are 27 independent error terms, at least 27 free parameters are required to fully cancel the error.

Again following Ref. [44], we choose to use a family of interrupted identity operations. For a single qubit, such an operation consists of a 2π rotation at one value of J interrupted by a 2π rotation at a different value of J. This second, inner 2π rotation can again be interrupted, and so forth for arbitrarily many 2π rotations. The free parameters in this family of operations include the values of J as well as the angles at which the interruptions take place. In this way, a family of identity operations which depends on any number of parameters can be generated. It is then simply a matter of extending this notion to a system of two qubits. We first address the case where $h_1 = h_2$, and then discuss the subtleties which arise when h_1 and h_2 are different.

A. Identity with $h_1 = h_2$

A naïve approach to finding an interrupted identity for two qubits would be to use a different sequence of interrupted 2π rotations on each qubit. There is, however, one major problem with such a scheme: the time taken to perform a 2π rotation depends on the value of J, so the portion of the first sequence which coincides with a part of the second sequence is also dependent on the values J takes. Then, for completely arbitrary parameters, it is not possible to find a simple general expression for the total error. We illustrate this problem with an example shown in Fig. 1. On each side is shown a pulse consisting of three 2π rotations on each qubit. In practice, these would be nested, but we use consecutive 2π rotations for the sake of this discussion. The total error would be a modified sum of the Δ_R terms using Eq. (23). The problem is that the arguments of Δ_R themselves are different for different values of j_n. For example, the term $\Delta_R(j_1, j_6)$ appears on the left of Fig. 1 but not the right, and $\Delta_R(j_3, j_4)$ appears on the right but not the left. Thus, while this is a perfectly valid uncorrected identity operation, in practice it would be very difficult to tune the parameters j_n to cancel a given error matrix due to the difficulty of finding a closed-form expression that is valid for all choices of j_n.

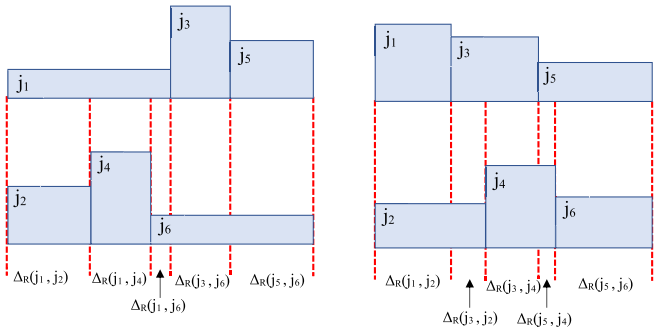

FIG. 1. Left: a naïve uncorrected identity operation consisting of a sequence of three 2π rotations on each of qubit 1 (top) and qubit 2 (bottom). Right: a similar uncorrected identity, but with different choices of the parameters $j_1 \ldots j_6$. As shown, the arguments of the error terms Δ_R are different for different values of $j_1 \ldots j_6$.

Theoretically, this is a perfectly allowed dynamical decoupling protocol, but numerically solving for the specific values of the parameters is challenging, if not impossible.

To circumvent this problem, an identity operation for the entire two-qubit system which has tunable parameters is required. Additionally, we require that it should not be symmetric between the two qubits since the errors accumulated on each qubit may differ. The simplest such identity operation consists of a pair of interrupted 2π rotations on one qubit, and one 4π rotation on the other, as shown in Fig. 2. The value of j' for the 4π rotation is chosen so that it takes the same amount of time as the two 2π rotations. Note that the condition $h_1 = h_2$ is implicitly used here since a value of j' which allows the pulses on each qubit to take the same time is not guaranteed to exist if h_1 and h_2 are not equal, as discussed in the next section. This identity operation can then be nested many times, alternating which qubit undergoes the 4π rotation and the two 2π rotations.

We now define $h_1 = h_2 = h$ to be the common value of h_1 and h_2. This situation is in fact typical for two-qubit experiments, with typical values of h being 30 MHz (Ref. [15]) and 23 MHz (Ref. [19]). We introduce the following notation in order to clearly define the nested identity operation discussed

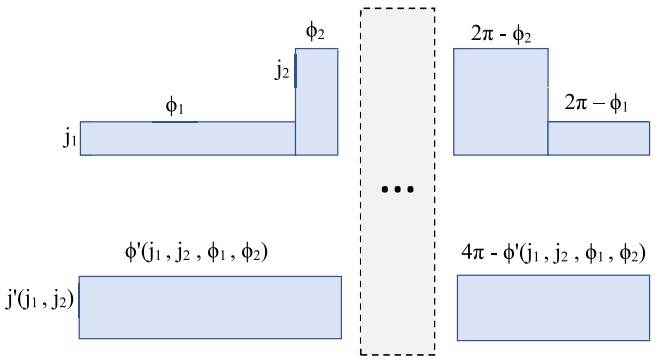

FIG. 2. An uncorrected identity for which a closed-form expression for arbitrary choices of the parameters is easy to obtain. There are four free parameters, namely, j_1, j_2, ϕ_1, and ϕ_2. The values of j' and ϕ' are determined by the other parameters.

above. Let $U(J_1, J_2, t)$ be an uncorrected rotation at values J_1 and J_2 for a time t. Also let $t(j,\phi)$ be the time required to perform a rotation by an angle of ϕ about the axis with the given value of j. Then, $t(j,\phi)$ is given as follows:

$$t(j,\phi) = \frac{\phi}{2\sqrt{h^2 + j^2}}, \tag{24}$$

Since our scheme requires alternating on which qubit the two 2π rotations are performed, we define the quantity $U_{(n)}(j,j',\phi)$ to encode this alternation. The notation corresponds to Fig. 2, where j gives the height of a particular 2π rotation, and ϕ gives the angle at which the rotation is interrupted, while j' is the value of the exchange coupling at which the other qubit is held during this rotation. Whether qubit 1 or 2 corresponds to j or j' is given by the parity of the subscript (n), so that in terms of $U(J_1, J_2, t)$ described above, $U_{(n)}(j,j',\phi)$ can be written as

$$U_{(n)}(j,j',\phi) = \begin{cases} U(j,j',t(j,\phi)) & \text{if } n \text{ is odd,} \\ U(j',j,t(j,\phi)) & \text{if } n \text{ is even.} \end{cases} \tag{25}$$

Because the total time taken to perform the two 2π rotations must equal the time required to perform the 4π rotation, the value j' at which the 4π rotation is performed must depend on the values of j chosen for the two 2π rotations. Thus, we define j'_n as the value needed in order to fulfill this condition in terms of the values j_{2n-1}, j_{2n}, and find that j'_n is given as follows:

$$j'_n = \sqrt{-1 + \left(\frac{2\pi}{t(j_{2n-1},2\pi) + t(j_{2n},2\pi)}\right)^2}. \tag{26}$$

One level of the identity operation consists of four rotations, as shown in Fig. 2. Nesting N copies of this identity will then result in a product of $2N$ partial 2π rotations followed by the product of the $2N$ completions of these rotations in the reverse order. Thus, in terms of our previous notation, an Nth level nested uncorrected identity denoted $I^{(N)}$ is given by

$$\begin{aligned} I^{(N)} = &\prod_{n=1}^{N} [U_{(n)}(j_{2n-1}, j'_n, \phi_{2n-1}) U_{(n)}(j_{2n}, j'_n, \phi_{2n})] \\ &\times \prod_{n=N}^{1} [U_{(n)}(j_{2n}, j'_n, 2\pi - \phi_{2n}) \\ &\times U_{(n)}(j_{2n-1}, j'_n, 2\pi - \phi_{2n-1})]. \end{aligned} \tag{27}$$

This method can correct to first order any single-qubit gate or product of single-qubit gates. As a demonstration of this procedure, we provide pulse sequences for gates of the form $R \otimes 1$, where R is one of the 24 Clifford gates. To implement this method of deriving dynamical pulse sequences, we first find short uncorrected pulse sequences which implement the desired gates. Reference [45] covers this topic in great detail, and we use the equations for implementing arbitrary rotations found there, many of which have extra degrees of freedom. (We refer to Ref. [45] for the necessary technical details here.) In principle, these degrees of freedom could be added to the list of free parameters j_i, ϕ_i in the uncorrected identity operation, possibly resulting in a marginally more optimal pulse sequence. However, these extra parameters are gate

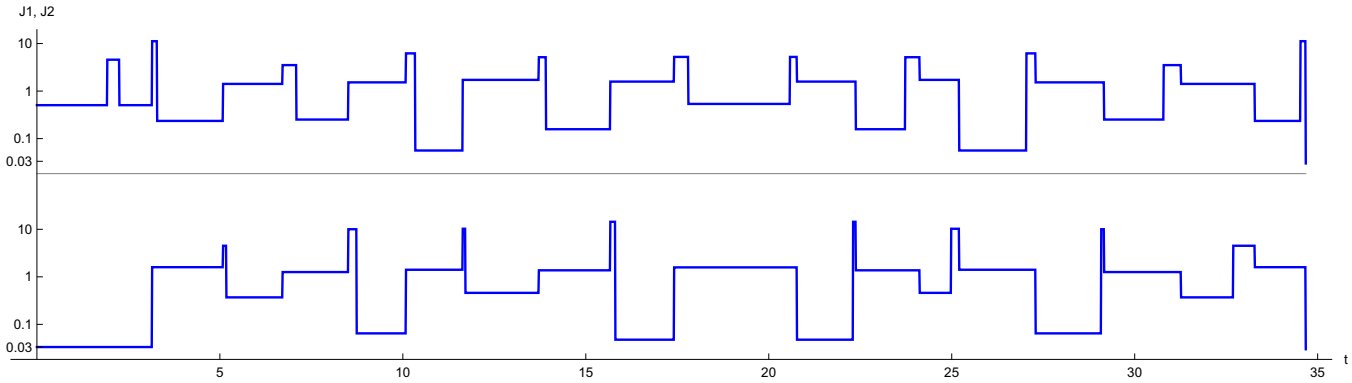

FIG. 3. A corrected pulse implementing a π rotation about the $x+y$ axis. J_1 (top) and J_2 (bottom) are plotted against time, with $h_1 = h_2 = 1$.

dependent, and so in order to treat all gates identically, we make arbitrary choices for these parameters, giving preference to choices which have low values of J_1 or J_2 since the strength of the capacitive coupling is proportional to J_1 and J_2. During this initial rotation sequence, which is performed on qubit 1, we perform a single uncorrected $2n\pi$ rotation at constant J_2 on the qubit 2, with J_2 and n chosen so that the total time of the initial pulse sequence and the $2n\pi$ rotation are the same.

After calculating the error Δ_{rot} using Eqs. (18) and (21), we construct an uncorrected identity of the form given in Eq. (27). Since 27 parameters are needed, at least a level 7 uncorrected identity is required; however, we have used a level 9 identity in order to introduce extra parameters, which helps the numerical methods used to solve the equations converge more quickly and consistently. In particular, we minimize the norm of the sum $\Delta_{\text{rot}} + \Delta_{\text{idt}}$. A local minimization technique is used which requires initial values for the parameters, and a poor choice of these values can cause the method to converge to a local minimum not equal to zero. We find that choosing j_i to have magnitudes alternating between large ($j_{2n-1} > h$) and small ($j_{2n} < h$), and choosing ϕ_i close to π generally give good results. We leave some room for variation, pseudorandomly generate many sets of values of j_i and ϕ_i, and use for the set of initial values the one which gives the smallest norm of $\Delta_{\text{rot}} + \Delta_{\text{idt}}$. During this minimization, we require that $j_{\min} \leqslant j_i \leqslant j_{\max}$, with $j_{\min}$ and $j_{\max}$ equal to $\frac{1}{30}h$ and $30h$, respectively. These values have been chosen to approximate current experimental capabilities [52]. Our method works with tighter constraints, though a higher level identity (longer pulse) may be required to find a solution.

B. Constraints with $h_1 \neq h_2$

We now address the case where h_1 and h_2 differ by a known amount Δh greater than dh_1, dh_2, so that terms second order in Δh cannot be ignored (if $\Delta h \ll 1$, then we can simply treat $h_1 = h_2$ and let Δh be absorbed into the dh_1 and dh_2 error terms). We can use a similar method as in subsection A above, with Eq. (24)–(26) becoming

$$h_{(n)} = \begin{cases} h_1 & \text{if } n \text{ is odd,} \\ h_2 & \text{if } n \text{ is even,} \end{cases} \tag{28}$$

$$t_{(n)}(j,\phi) = \frac{\phi}{2\sqrt{h_{(n)}^2 + j^2}}, \tag{29}$$

$$U_{(n)}(j,j',\phi) = \begin{cases} U(j,j',t_{(n)}(j,\phi)) & \text{if } n \text{ is odd,} \\ U(j',j,t_{(n)}(j,\phi)) & \text{if } n \text{ is even,} \end{cases} \tag{30}$$

$$j'_n = \sqrt{-h_{(n+1)}^2 + \left[\frac{2\pi}{t_{(n)}(j_{2n-1},2\pi) + t_{(n)}(j_{2n},2\pi)}\right]^2}. \tag{31}$$

Here, parentheses (n) in the subscript denote that only the parity of n is important and not its value.

The difficulty lies in ensuring that all values of j_i and j'_i are bounded between $j_{\min}$ and $j_{\max}$. When $h_1 = h_2$, the constraints $j_{\min} \leqslant j_i \leqslant j_{\max}$ automatically enforce $j_{\min} \leqslant j' \leqslant j_{\max}$; however, when $h_1 \neq h_2$, additional constraints are needed. We approach this problem by noticing that Eq. (31) is symmetric between j_{2n-1} and j_{2n}. This initially motivates us to require that the constraints on j_{2n-1} and j_{2n} be identical as well. This simplifies the initial calculations, but we also address allowing asymmetric constraints between j_{2n-1} and j_{2n}. Solving Eqs. (29) and (31) along with the inequality, $j_{\min} \leqslant j' \leqslant j_{\max}$, we find the following constraints on j_i:

$$\sqrt{j_{\min}^2 - h_{(n)}^2 + h_{(n+1)}^2} \leqslant j_{2n-1}, j_{2n},$$
$$j_{2n-1}, j_{2n} \leqslant \sqrt{j_{\max}^2 - h_{(n)}^2 + h_{(n+1)}^2}. \tag{32}$$

In practice, $j_{\max} \gg h_1, h_2$, so the maximum $\sqrt{j_{\max}^2 - h_{(n)}^2 + h_{(n+1)}^2} \approx j_{\max}$, and thus can be ignored. The minimum is also ignored when $-h_{(n)}^2 + h_{(n+1)}^2 < 0$ since $j_i \geqslant j_{\min}$ fulfills this inequality also. This occurs for all odd or even n depending on whether h_1 or h_2 is larger. Using this additional constraint, the same process described above is used to find a pulse sequence, though a longer pulse may be necessary due to the tighter constraints.

Since the pulse sequences we find generally consist of values j_i alternating between large and small (due to our choice of starting values during the minimization process), it is natural to consider allowing $j_{2n} \geqslant j_{\min}$ and deriving the minimum constraint on j_{2n-1}, which yields

$$j_{2n-1} \geqslant \left[-h_{(n)}^2 + \frac{\left(h_{(n+1)}^2 + j_{\min}^2\right)\left(h_{(n)}^2 + j_{\min}^2\right)}{\left(2\sqrt{h_{(n)}^2 + j_{\min}^2} - \sqrt{h_{(n+1)}^2 + j_{\min}^2}\right)^2}\right]^{1/2}. \tag{33}$$

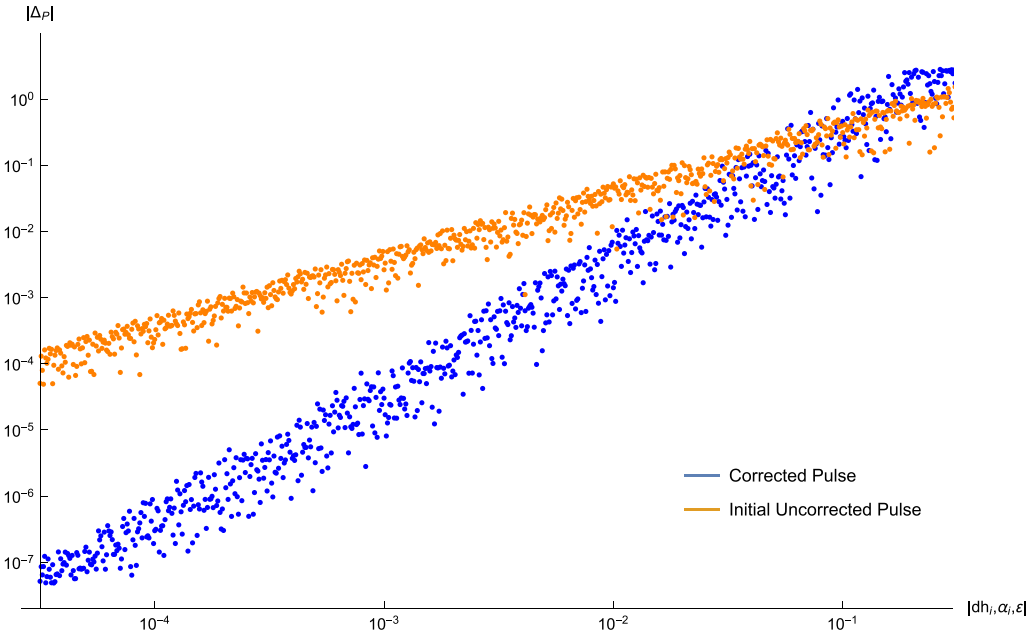

FIG. 4. The total error of corrected (blue) and uncorrected (orange) pulses versus the norm of dh_i, α_i, ε. It is clear from the slopes of the lines that the uncorrected pulse error is first order and the corrected pulse error is second order in dh_i, α_i, ε.

Assuming $j_{\min} \ll h_1, h_2$, this simplifies to

$$j_{2n-1} \geqslant \frac{2h_{(n)}^{3/2}\sqrt{h_{(n+1)} - h_{(n)}}}{2h_{(n)} - h_{(n+1)}}. \tag{34}$$

This approach is only valid for $h_{(n+1)} < 2h_{(n)}$. For differences greater than this, a different choice of uncorrected identity is needed, which, although possible, is beyond the scope of this work.

C. Results

Parameters for the corrected pulse sequences for the 24 Clifford gates for the case where $h_1 = h_2 = 1$ are given in Appendix A. We have also considered the simple situation in which, rather than setting $dJ_i = \alpha_i J_i$, with α_i a small constant, we simply let dJ_i be constant for the duration of the sequence, and provided parameters for the resulting corrected sequences in Appendix B. The top portions of the tables give the parameters j'^{rot}, j_i^{rot}, and t_i^{rot} for the initial uncorrected rotations,

$$U^{\text{rot}} = \prod_i U\left(j_i^{\text{rot}}, j'^{\text{rot}}, t_i^{\text{rot}}\right), \tag{35}$$

and the bottom portions give the parameters j_i and ϕ_i for the uncorrected identity $I^{(9)}$ given by Eq. (27). As an example, we plot the error-corrected pulse sequence for the gate $e^{-\frac{i}{2}\frac{X+Y}{\sqrt{2}}\pi}$ in Fig. 3.

To precisely quantitatively calculate the fidelity of the dynamically corrected gate operations using our pulse sequences starting with given error sets, a detailed randomized benchmarking analysis is necessary. Such a randomized benchmarking analysis, which is better done in connection with the actual experimental work implementing our pulse sequences in the ST qubit gate operations, is well beyond the scope of this work. However, it is easy to show that the errors in the sequences we found are second order in dh_i, α_i, and ε, given that these values are constant, i.e., these sequences correct noise- and crosstalk-induced error to leading order. For a given pulse sequence and a set of values dh_i, α_i, and ε, we can evaluate e^{-itH} for each rotation in the pulse sequence using the full Hamiltonian with errors given in Eq. (19). By combining these rotations with error and comparing to the ideal rotation, the total error of the pulse sequence $\Delta_P(dh_i, \alpha_i, \varepsilon)$ can be determined for the given values of dh_i, α_i, and ε. Taking the norm of Δ_P, defined as $|\Delta_P| = \sqrt{\text{Tr}\,\Delta_P^\dagger \Delta_P}$, we have measure of the error of a given pulse sequence. For each sequence, we generate many sets of values dh_i, α_i, and ε, and plot $|\Delta_P|$ against the norm of $(dh_1, dh_2, \alpha_1, \alpha_2, \varepsilon)$, and find that the total error is clearly second order in dh_i, α_i, and ε. We show an example of such a plot, in this case for the gate $e^{\frac{-i}{2}\frac{X+Y}{\sqrt{2}}\pi}$, in Fig. 4. We generate plots like this for all 24 pulses and find that they are qualitatively identical to the one shown. As can be seen from Fig. 4, an initial error of 10^{-3} can be corrected by two or three orders of magnitude by our pulse sequence whereas the corresponding error correction for starting errors of 10^{-1} is more modest (in the range of one order of magnitude or less). A full randomized benchmarking analysis is likely to give numbers close to these direct estimates based on specific pulse sequences. If the uncorrected system has a fidelity of 95%, our dynamical decoupling scheme should be able to improve the fidelity to well above 99%, but a starting fidelity of 90% may be too low for our scheme to improve it above 99%. It is also important to note that although our scheme corrects quite well against correlated errors, if the system is dominated by white noise or uncorrelated errors, uncorrected pulses are still favorable. Notably this sets limits on the minimum precision needed to implement the corrected gates. In particular, a precision of at least 0.1% for each of the parameters is needed in order for the corrected pulses to offer an advantage over the uncorrected gates.

IV. CONCLUSION

We have addressed the issue of crosstalk between two capacitively coupled singlet-triplet qubits. While such a coupling is necessary to perform multiqubit operations, it also has a detrimental effect on single-qubit operations: it causes unintentional rotation of the other qubit(s), and also causes errors in the intentional rotation of the qubit under consideration. As a result, it is crucial to develop a method for correcting for not only noise-induced error, but for crosstalk-induced error as well. Our proposed dynamical decoupling scheme does this precisely. Our method is a generalization of the SUPCODE technique of Refs. [43–45]. We first perform our naïve pulse sequence for implementing a given single-qubit gate, followed by an uncorrected identity operation with its parameters arranged in such a way as to cancel the effects of noise and crosstalk to leading order. Unlike in the single-qubit case already considered in the literature, the case of two capacitively coupled qubits provides additional challenges. Because of the fact that the capacitive coupling is proportional to the exchange couplings of the two qubits, we cannot make these couplings too large, lest we make the capacitive coupling, and thus the crosstalk, large as well. We must also ensure that the pulse sequences applied to each qubit take the same amount of time to complete. Our method for implementing the uncorrected identity, in which we divide the identity into segments within which one qubit is subject to two pulses and the other to just one of identical duration, allows us to address both of these issues. We provide an analysis of one of the pulse sequences that results from this procedure, namely, that of a rotation by π about the $\hat{\hat{x}} + \hat{\hat{y}}$ axis, and also provide parameters for all 24 of the Clifford gates used in randomized benchmarking simulations in the Appendix. We also show that these pulses, as claimed, do indeed cancel the error in the naïve pulse sequences to leading order by plotting the error as a function of the noise and crosstalk strength. Throughout, we assume upper and lower bounds on the exchange couplings that approximate experimental constraints.

All of the results that we provide assume that the magnetic field gradient on the two qubits is the same for both. It is entirely possible for the gradients to differ. While our sequences can correct for small variations due to imperfections in fabrication of the micromagnets or polarization of the nuclei used to realize the gradients (we simply add them to the error terms), we do not derive results for cases in which the difference in the gradient between the two qubits is significant, whether by design or by accident. We have, however, provided some discussion of this case; we showed that additional complications arise, in the form of tighter constraints on the allowed exchange coupling strengths than we would expect entirely from experimental constraints. We also note that, throughout this work, we assumed that the noise in the system is quasistatic. While this is often a good approximation [19], the noise in actual experimental systems is known to follow a power-law spectrum [16,53] ($1/f^{\alpha}$). We see, however, from the previous work [44,45] that, even in this scenario, similar approaches to that which we adopt here to combat the effects of noise still result in noticeable improvement in gate fidelities. We thus expect similar results for the capacitively coupled qubits considered here.

We also note that capacitive coupling is not the only type of coupling that can be realized between two singlet-triplet qubits. Exchange coupling is another type of coupling that can exist; we simply couple one quantum dot from one qubit to a quantum dot in the other qubit using a Heisenberg exchange interaction. This can be realized experimentally using a four-quantum-dot device operated as two singlet-triplet qubits, with the "middle" potential barrier used to control the exchange coupling between the qubits. This offers two advantages, but also a drawback. First of all, this type of coupling enables us to control the coupling of the qubits independently of the intraqubit exchange couplings, unlike capacitive coupling, which depends on the intraqubit exchange couplings. Second of all, it is compatible with the barrier, or symmetric, control scheme demonstrated in Ref. [19], which results in an order of magnitude less charge noise than tilt control. Realizing the capacitive coupling studied in this work, on the other hand, requires us to tilt the potential profile in order to produce the electric dipole moments needed. Therefore, we expect that a putative set of dynamically corrected pulse sequences for implementing single-qubit gates on exchange-coupled singlet-triplet qubits would avoid a number of the issues that arise with capacitively coupled qubits; we would no longer be required to use tilt control, thus allowing us to mitigate the effects of charge noise, and we would be able to use faster pulses. However, the disadvantage is that exchange coupling introduces yet another source of error beyond crosstalk, namely, leakage errors. It is possible for this coupling to take the qubits out of their logical subspace; for example, it could leave one qubit in the $|\uparrow\uparrow\rangle$ state and the other in the $|\downarrow\downarrow\rangle$ state. This would present an additional challenge to overcome in developing dynamically corrected pulse sequences for such a system. While a study of error correction in exchange-coupled singlet-triplet qubits would be interesting, it is beyond the scope of this work. In the end, whether capacitive coupling or exchange coupling is a better avenue for future progress in ST qubits depends quite a bit not only on the details of the noise and crosstalk in the systems, but also on the experimental ability to control the leakage error. We mention in this context that the capacitively coupled ST qubits are the only semiconductor spin-qubit systems to have demonstrated two-qubit gate-controlled operations, leading to our decision to study the ST qubits in depth in this work.

In conclusion, we have developed detailed dynamical decoupling pulse sequences for suppressing crosstalk and noise errors in capacitively coupled singlet-triplet spin qubits and have explicitly demonstrated their efficacy by showing that the corrected sequences manifest orders of magnitude lower errors than the naïve uncorrected sequences.

ACKNOWLEDGMENTS

The authors thank J. Kestner for helpful discussions. This work is supported by Laboratory for Physical Sciences.

APPENDIX A: TABLES OF DYNAMICALLY CORRECTED PULSE SEQUENCE PARAMETERS

We present here the parameters for the dynamically corrected pulse sequences that we have derived. The complete

TABLE I. Parameters for the dynamically corrected identity operation, the x and y rotations, and the z rotation by $\frac{\pi}{2}$.

Axis		x	x	x	y	y	y	z
Angle	Identity	$\pi/2$	π	$3\pi/2$	$\pi/2$	π	$3\pi/2$	$\pi/2$
j'^{rot}	0.03333	0.03333	0.03333	0.03333	0.03333	0.03333	0.03333	0.03333
j_1^{rot}	0.03333	0.03333	0.03333	0.03333	6.43043	7.31731	8.19725	1.00000
j_2^{rot}		0.88348	1.73498	3.88089	0.73084	0.75954	0.78254	0.21835
j_3^{rot}		0.03333	0.03333	0.03333	6.43043	7.31731	8.19725	1.00000
j_4^{rot}					0.73084	0.75954	0.78254	
j_5^{rot}					6.43043	7.31731	8.19725	
t_1^{rot}	3.13985	0.40660	0.79532	1.18104	0.12069	0.10635	0.09511	0.61342
t_2^{rot}		2.32664	1.54921	0.77777	1.26821	1.25089	1.23705	1.91300
t_3^{rot}		0.40660	0.79532	1.18104	0.12069	0.21269	0.28532	0.61342
t_4^{rot}					1.26821	1.25089	1.23705	
t_5^{rot}					0.36206	0.31904	0.28532	
j_1	4.25455	8.64919	8.97960	11.2324	4.69870	11.7867	16.5123	2.69759
j_2	0.09332	0.23284	0.05770	0.15526	0.45052	0.04100	0.28630	0.18032
j_3	8.02055	2.50370	10.2303	10.1333	14.3073	19.4429	3.79908	20.4549
j_4	0.06985	0.39326	0.08544	0.13815	0.06080	0.05751	0.35525	0.07026
j_5	10.6268	4.16386	4.11884	3.33988	7.62621	16.7854	4.50812	12.0166
j_6	0.21389	0.17203	0.06055	0.07889	0.55734	0.32611	0.04356	0.39711
j_7	7.37015	5.72370	3.90696	2.96801	8.28095	16.3807	9.11133	3.51155
j_8	0.08986	0.05960	0.26106	0.09212	0.05088	0.03886	0.26085	0.10698
j_9	7.64161	3.82995	2.06453	6.86584	4.04735	25.1775	6.51133	5.49661
j_{10}	0.17317	0.07476	0.08354	0.05764	0.67310	0.06981	0.05847	0.10551
j_{11}	4.66221	11.8434	12.2670	7.57279	15.3226	21.3511	5.54262	6.12039
j_{12}	0.13532	0.28465	0.16320	0.30184	0.08241	0.05312	0.56561	0.08912
j_{13}	6.51752	9.38462	8.88344	3.45868	3.78001	2.49265	5.73037	7.88694
j_{14}	0.06160	0.07390	0.06824	0.17500	0.11185	0.34648	0.06432	0.20510
j_{15}	9.20117	6.50713	8.40965	7.15013	6.01842	5.86112	9.20095	11.0451
j_{16}	0.06356	0.09257	0.35852	0.13261	0.31594	0.11879	0.07149	0.07399
j_{17}	4.56705	7.29008	9.44018	6.36630	8.37878	15.1228	21.0147	7.51700
j_{18}	0.09158	0.42999	0.11956	0.26920	0.46082	0.31023	0.05848	0.27828
ϕ_1	2.55322	4.66206	0.30870	4.51951	5.52197	3.64920	2.80854	3.21494
ϕ_2	3.00455	3.23089	2.12926	2.05844	5.00581	2.83173	4.02044	4.77361
ϕ_3	3.33459	4.11162	3.92240	4.21749	4.04230	3.18274	1.71682	2.38512
ϕ_4	2.96052	2.88401	4.33729	3.53703	2.73821	3.72700	3.01457	3.57115
ϕ_5	5.09619	3.21946	1.39096	2.21303	2.27049	0.92820	3.71351	3.80415
ϕ_6	2.33360	3.35709	3.42368	3.34577	4.07169	3.89570	2.73709	2.63703
ϕ_7	5.20802	1.84857	3.66689	4.25246	3.76942	2.01892	4.46601	2.88075
ϕ_8	3.71262	3.47093	2.51816	1.64612	3.20440	2.61221	2.86863	3.03145
ϕ_9	0.46072	3.30053	2.09375	2.84958	1.39429	4.71962	4.02309	3.03890
ϕ_{10}	3.39227	3.37554	3.27396	3.30266	3.68709	3.88283	3.29495	2.73878
ϕ_{11}	2.55021	5.62423	1.71873	1.59029	1.43437	2.62054	0.18895	5.34732
ϕ_{12}	2.65459	1.74187	4.45157	4.16496	4.23973	2.57055	4.15438	3.30636
ϕ_{13}	5.21937	4.40566	2.93057	2.22547	2.23942	2.75109	3.17595	5.68995
ϕ_{14}	2.91567	2.92878	2.85932	3.42050	2.13964	2.91979	2.97230	1.91518
ϕ_{15}	3.79412	2.44601	4.29348	3.91960	4.96730	3.87946	3.41412	4.76460
ϕ_{16}	2.13795	2.96169	3.57123	2.51887	2.08244	2.82506	3.57640	2.60517
ϕ_{17}	4.12557	2.35265	0.43890	4.22659	5.48983	3.28908	2.47360	2.86459
ϕ_{18}	3.14159	3.14159	3.14159	3.14159	3.14159	3.14159	3.14159	3.14159

pulses are given by Eqs. (35) and (27) with parameters given in Tables I–III. All j values are in units of h.

APPENDIX B: DYNAMICALLY CORRECTED PULSE PARAMETERS FOR CONSTANT dJ_i

Throughout this work, in the main text, we have used a model where dJ_i is proportional to J_i. However, other models may exist, and the numerics of our method are able to generate pulse sequences for a range of different models. To demonstrate this, we also derived pulse sequences for the case where dJ_i is independent of J_i, and found that these sequences also corrected first-order error in the model chosen. The parameters for these sequences are given in Tables IV–VI. In principle, if experiments warrant generating dynamical decoupling pulse

TABLE II. Parameters for the dynamically corrected z rotations by π and $3\pi/2$, and for the rotations by $\hat{x}\pm\hat{y}$, $\hat{x}\pm\hat{z}$, and $\hat{y}\pm\hat{z}$.

Axis	z	z	$\hat{x}+\hat{y}$	$\hat{x}-\hat{y}$	$\hat{x}+\hat{z}$	$\hat{x}-\hat{z}$	$\hat{y}+\hat{z}$	$\hat{y}-\hat{z}$
Angle	π	$3\pi/2$	π	π	π	π	π	π
j'^{rot}	0.03333	0.03333	0.03333	0.03333	2.64575	0.57485	0.03333	0.03333
j_1^{rot}	2.00000	3.00000	0.50509	0.50509	1.00000	2.53276	1.71541	1.71541
j_2^{rot}	0.45510	0.67658	4.57172	4.57172		0.03333	0.13012	0.13012
j_3^{rot}	2.00000	3.00000	0.50509	0.50509		2.53276	1.71541	1.71541
j_4^{rot}								
j_5^{rot}								
t_1^{rot}	0.50027	0.42475	1.91411	0.89008	1.11072	0.57686	0.51303	1.06916
t_2^{rot}	2.13931	2.29036	0.33565	0.33565		1.56992	1.55767	1.55767
t_3^{rot}	0.50027	0.42475	0.89008	1.91411		0.57686	1.06916	0.51303
t_4^{rot}								
t_5^{rot}								
j_1	14.9279	23.9766	11.2197	5.88326	0.96910	4.21145	7.89663	10.5977
j_2	0.21741	0.08751	0.23548	0.06925	0.33248	0.04880	0.16242	0.15088
j_3	2.80327	12.5873	4.50703	6.85985	10.5444	3.73761	9.24311	4.57720
j_4	0.24971	0.29095	0.36990	0.19478	0.08280	0.20116	0.05004	0.14168
j_5	13.6280	5.05654	3.51726	3.10676	8.22643	6.15100	11.9739	11.9299
j_6	0.11850	0.12464	0.25159	0.12773	0.41291	0.07436	0.37828	0.04724
j_7	5.43618	10.4596	10.0448	6.14212	10.9543	6.86964	3.16910	11.1235
j_8	0.19053	0.16828	0.06464	0.10770	0.05153	0.10872	0.09210	0.19887
j_9	2.93129	25.2507	6.21325	3.62073	3.99054	5.02616	5.40783	8.30899
j_{10}	0.17401	0.24332	0.05614	0.04634	0.56279	0.30939	0.24328	0.23214
j_{11}	5.34895	13.9661	10.2701	7.06335	1.16160	19.2500	12.1845	10.3575
j_{12}	0.40949	0.45280	0.45991	0.30292	0.04781	0.12683	0.08331	0.32868
j_{13}	22.1116	19.8886	5.15864	5.85519	5.87043	19.8651	3.88747	9.48442
j_{14}	0.04834	0.04964	0.15747	0.13325	0.21666	0.06943	0.15774	0.07721
j_{15}	8.28348	20.8913	14.3910	4.07973	7.49208	7.38150	14.5753	6.62029
j_{16}	0.03776	0.08864	0.04757	0.06969	0.04560	0.04795	0.08895	0.08536
j_{17}	17.3790	11.8760	5.23171	7.38525	11.1053	9.76455	5.52560	9.49243
j_{18}	0.28731	0.13834	0.53640	0.31872	0.06706	0.20667	0.56000	0.16461
ϕ_1	0.17390	4.46173	3.23390	2.22917	3.39790	5.28562	0.65047	0.63295
ϕ_2	3.09168	2.33997	3.70695	3.85984	3.95766	3.62949	2.92893	3.60713
ϕ_3	3.07075	4.39117	0.80794	2.98899	4.26243	1.80037	3.38641	2.60625
ϕ_4	3.39482	3.60846	3.26099	2.19380	3.35828	3.33234	2.88631	2.80943
ϕ_5	2.93283	2.65185	2.77504	4.15096	1.54770	2.81655	2.51553	4.12300
ϕ_6	2.65427	3.56274	2.93110	3.34935	3.91568	2.96830	3.16500	2.66819
ϕ_7	4.87590	0.86494	4.65637	1.82555	1.90529	3.86311	4.43373	5.59828
ϕ_8	2.51402	3.42610	2.69527	3.99554	3.59852	3.47884	2.45794	2.53965
ϕ_9	4.14460	2.17747	3.14723	3.55778	2.34369	2.19616	5.64073	4.45949
ϕ_{10}	3.45194	3.09249	2.60268	3.09779	4.24466	3.00242	3.21892	3.53377
ϕ_{11}	0.26740	5.38412	1.58592	5.06376	0.79352	6.05802	3.55833	0.49920
ϕ_{12}	3.84950	2.68984	4.40648	2.19840	2.86710	3.79569	2.95205	3.42713
ϕ_{13}	2.66076	3.07483	2.14367	3.92841	5.36926	2.38004	2.08220	2.48413
ϕ_{14}	3.27057	3.42195	3.54935	3.08201	1.77750	3.01509	3.04083	3.12396
ϕ_{15}	2.94726	2.01300	3.96286	2.65718	4.68514	3.74243	3.17084	3.63762
ϕ_{16}	3.86814	2.82538	3.21533	2.96932	2.63704	3.38304	3.75684	3.40975
ϕ_{17}	3.27372	3.39624	4.21481	2.24716	3.60030	4.05433	3.12939	3.00546
ϕ_{18}	3.14159	3.14159	3.14159	3.14159	3.14159	3.14159	3.14159	3.14159

sequences for other possible coupling models for ST qubits, our method can easily be generalized to handle such scenarios.

As in the previous set of tables, all j values are in units of h.

TABLE III. Parameters for the dynamically corrected $\hat{x} \pm \hat{y} \pm \hat{z}$ rotations.

Axis	$\hat{x}+\hat{y}+\hat{z}$	$\hat{x}+\hat{y}+\hat{z}$	$-\hat{x}+\hat{y}+\hat{z}$	$-\hat{x}+\hat{y}+\hat{z}$	$\hat{x}-\hat{y}+\hat{z}$	$\hat{x}-\hat{y}+\hat{z}$	$\hat{x}+\hat{y}-\hat{z}$	$\hat{x}+\hat{y}-\hat{z}$
Angle	$2\pi/3$	$4\pi/3$	$2\pi/3$	$4\pi/3$	$2\pi/3$	$4\pi/3$	$2\pi/3$	$4\pi/3$
j'^{rot}	0.03333	0.03333	0.03333	0.03333	0.03333	0.03333	0.03333	0.03333
j_1^{rot}	0.56170	0.74456	0.32145	0.29210	0.56170	0.74456	0.29210	0.32145
j_2^{rot}	2.41400	3.22657	14.0228	8.36716	2.41400	3.22657	8.36716	14.0228
j_3^{rot}	0.56170	0.74456	0.32145	0.29210	0.56170	0.74456	0.29210	0.32145
j_4^{rot}								
j_5^{rot}								
t_1^{rot}	2.21343	1.97092	1.17574	1.18212	0.52564	0.54891	1.83346	1.81513
t_2^{rot}	0.40078	0.62001	0.14898	0.12427	0.40078	0.62001	0.12427	0.14898
t_3^{rot}	0.52564	0.54891	1.81513	1.83346	2.21343	1.97092	1.18212	1.17574
t_4^{rot}								
t_5^{rot}								
j_1	3.53560	7.40870	9.30530	6.38544	10.7248	17.2594	7.05950	15.1935
j_2	0.23139	0.10157	0.11817	0.12981	0.21240	0.17560	0.32670	0.11769
j_3	16.0966	6.97001	10.6390	6.51320	3.11017	27.1973	1.29162	9.17358
j_4	0.07111	0.11694	0.08366	0.18193	0.14994	0.03927	0.32813	0.11144
j_5	19.3300	4.58619	6.75684	5.18100	18.7600	5.91114	3.97861	8.94809
j_6	0.16332	0.06442	0.21631	0.12154	0.07568	0.37476	0.13895	0.33521
j_7	19.2548	5.60181	8.66110	4.18403	12.5498	7.98067	5.94619	12.1638
j_8	0.04468	0.17014	0.14226	0.18787	0.29095	0.03475	0.05824	0.13070
j_9	13.7738	13.4672	18.4340	3.59364	6.79908	11.9460	3.70590	19.3022
j_{10}	0.08073	0.13413	0.24654	0.04273	0.15602	0.31084	0.04433	0.20006
j_{11}	5.95821	7.28592	10.7813	6.93732	6.81217	8.42940	8.91232	6.86166
j_{12}	0.13448	0.40891	0.15650	0.33408	0.31731	0.05540	0.33998	0.06192
j_{13}	11.2806	7.39708	7.60260	4.74451	8.48105	21.8867	3.84464	5.46750
j_{14}	0.16682	0.05707	0.30270	0.05037	0.09169	0.16977	0.05388	0.27407
j_{15}	21.0041	11.2817	15.3315	5.09639	4.75689	12.7137	6.22348	4.54025
j_{16}	0.12130	0.06069	0.05541	0.04628	0.08300	0.37435	0.08023	0.06762
j_{17}	14.7728	8.14723	7.37956	6.53512	11.0940	3.36556	7.16938	22.1340
j_{18}	0.17654	0.17674	0.24785	0.21341	0.13782	0.05163	0.51527	0.21191
ϕ_1	2.53825	4.38397	2.65058	2.65215	2.00758	2.68429	5.33741	3.85920
ϕ_2	4.53270	2.20273	2.38158	2.35687	3.52438	2.75927	3.86201	3.37853
ϕ_3	2.59203	4.26832	4.80735	3.92194	2.59147	3.31991	2.81744	2.98401
ϕ_4	3.75470	3.80220	3.24547	3.85075	3.15874	3.39732	2.94563	3.31101
ϕ_5	0.52120	1.79639	2.94582	2.19146	3.34913	2.54966	3.55481	5.69859
ϕ_6	2.78943	3.64199	2.46653	2.92552	2.74580	3.66193	3.26094	3.42371
ϕ_7	2.39957	0.94526	3.64461	4.13605	5.08724	4.01620	1.84110	3.02494
ϕ_8	3.27728	3.49039	3.53042	2.31790	2.53522	2.67545	3.44628	2.23430
ϕ_9	4.13341	2.34697	1.92427	3.04953	4.33241	5.72953	3.24584	5.21972
ϕ_{10}	3.64683	2.75723	2.99155	3.37997	3.63580	2.60940	3.40564	1.96004
ϕ_{11}	4.64988	5.83925	5.29808	0.84137	0.28982	4.63477	5.17615	3.73298
ϕ_{12}	2.94845	2.76326	3.73889	4.18084	3.55508	2.69058	1.48630	2.67019
ϕ_{13}	6.10583	3.74351	3.17347	1.99631	2.54828	3.63376	3.93282	4.10101
ϕ_{14}	3.47632	3.35216	2.89166	3.62070	3.25964	2.74220	3.41431	3.90467
ϕ_{15}	1.43617	2.16943	3.31085	2.91108	2.93229	3.16477	1.31813	2.69967
ϕ_{16}	3.36972	3.06705	3.20338	3.46981	3.72947	4.28321	3.27278	3.30133
ϕ_{17}	3.62018	3.37820	2.73933	4.06683	3.07756	0.25141	2.27238	5.24267
ϕ_{18}	3.14159	3.14159	3.14159	3.14159	3.14159	3.14159	3.14159	3.14159

TABLE IV. Parameters for the dynamically corrected identity operation, the x and y rotations, and the z rotation by $\frac{\pi}{2}$ for a model with constant J_i.

Axis		x	x	x	y	y	y	z
Angle	(Identity)	$\pi/2$	π	$3\pi/2$	$\pi/2$	π	$3\pi/2$	$\pi/2$
j'^{rot}	0.03333	0.03333	0.03333	0.03333	0.03333	0.03333	0.03333	0.03333
j_1^{rot}	0.03333	0.03333	0.03333	0.03333	6.43043	7.31731	8.19725	1.00000
j_2^{rot}		0.88348	1.73498	3.88089	0.73084	0.75954	0.78254	0.21835
j_3^{rot}		0.03333	0.03333	0.03333	6.43043	7.31731	8.19725	1.00000
j_4^{rot}					0.73084	0.75954	0.78254	
j_5^{rot}					6.43043	7.31731	8.19725	
t_1^{rot}	3.13985	0.40660	0.79532	1.18104	0.12069	0.10635	0.09511	0.61342
t_2^{rot}		2.32664	1.54921	0.77777	1.26821	1.25089	1.23705	1.91300
t_3^{rot}		0.40660	0.79532	1.18104	0.12069	0.21269	0.28532	0.61342
t_4^{rot}					1.26821	1.25089	1.23705	
t_5^{rot}					0.36206	0.31904	0.28532	
j_1	5.46325	4.79267	10.3137	19.4597	7.27643	14.6880	12.1954	18.8080
j_2	0.11660	0.34036	0.30761	0.09602	0.17189	0.05126	0.17555	0.07608
j_3	7.83045	9.43393	15.1785	3.35795	12.5444	4.86269	21.7404	1.77304
j_4	0.19007	0.05276	0.06575	0.04726	0.03873	0.06463	0.03914	0.15544
j_5	14.0880	8.39676	4.44094	12.2696	14.3122	20.8924	20.9836	11.8583
j_6	0.08858	0.55349	0.09376	0.06754	0.05058	0.29920	0.18160	0.08084
j_7	7.86256	7.36736	17.6563	4.50145	5.50740	4.24082	3.78485	5.78212
j_8	0.24579	0.05809	0.11776	0.20283	0.30428	0.06582	0.06840	0.09301
j_9	8.75655	4.55834	23.1891	6.27128	12.4862	6.52354	2.56912	5.09631
j_{10}	0.47191	0.48569	0.06621	0.21726	0.06858	0.44181	0.09971	0.33394
j_{11}	13.0447	8.70805	6.58776	14.2591	10.3155	11.3152	22.5411	5.15544
j_{12}	0.04996	0.04185	0.37826	0.24168	0.10836	0.23690	0.09658	0.33536
j_{13}	8.16027	3.65005	11.7940	5.28220	9.68209	15.1274	10.0745	2.95355
j_{14}	0.37463	0.45310	0.19711	0.12640	0.06406	0.12887	0.05410	0.07845
j_{15}	8.59080	3.72874	14.2332	21.4867	9.12064	23.7044	20.3803	4.59443
j_{16}	0.05091	0.09174	0.11715	0.07025	0.05448	0.05521	0.03650	0.06872
j_{17}	8.68563	3.72280	19.1950	13.6475	1.30298	18.1969	10.1510	9.98698
j_{18}	0.54697	0.74161	0.14063	0.08958	1.17119	0.55345	0.58051	0.44689
ϕ_1	3.77050	2.08723	4.87126	2.05446	3.66034	2.28203	1.37456	3.35636
ϕ_2	3.08246	2.19136	2.24372	2.08569	2.01941	2.62145	3.27109	2.90279
ϕ_3	3.04031	3.88529	4.54342	4.60125	3.91929	4.65150	0.50256	3.47771
ϕ_4	3.59030	3.15322	3.25836	3.34866	2.82642	3.34064	2.86164	2.84707
ϕ_5	0.55135	2.71164	2.55084	2.63841	2.92500	1.62537	2.72019	3.38188
ϕ_6	2.17272	2.90728	2.89031	2.54085	2.96817	3.28533	3.04122	3.85092
ϕ_7	4.89381	3.66293	2.01301	4.18211	1.81668	3.89362	3.95251	1.10297
ϕ_8	3.12411	2.66501	4.03373	2.10076	3.85824	2.42106	3.14859	3.67710
ϕ_9	3.16856	5.35428	0.91936	5.19087	1.22979	4.52306	4.46065	1.64572
ϕ_{10}	4.44070	2.98250	3.07860	2.49427	3.55619	1.78678	3.99485	3.08432
ϕ_{11}	3.43482	3.84937	5.27382	6.04607	4.11185	3.63263	1.15521	5.93853
ϕ_{12}	3.34802	2.63375	3.08498	2.94918	3.42171	2.58892	3.27690	2.30308
ϕ_{13}	1.45811	2.85588	3.78840	5.01766	3.12784	5.35763	1.04860	3.77584
ϕ_{14}	3.17489	3.53121	2.87810	2.81372	3.60913	3.02506	2.95315	3.03211
ϕ_{15}	3.22668	3.15860	2.59690	3.27866	0.85238	4.77421	2.49322	2.77818
ϕ_{16}	3.22662	3.09129	3.73021	2.69768	3.44236	2.88387	3.38333	2.69569
ϕ_{17}	4.00536	4.29243	1.89763	2.89193	3.21522	4.92074	4.01619	3.31403
ϕ_{18}	3.14159	3.14159	3.14159	3.14159	3.14159	3.14159	3.14159	3.14159

TABLE V. Parameters for the dynamically corrected z rotations by π and $3\pi/2$, and for the rotations by $\hat{x} \pm \hat{y}$, $\hat{x} \pm \hat{z}$, and $\hat{y} \pm \hat{z}$ for a model with constant J_i.

Axis	z	z	$\hat{x}+\hat{y}$	$\hat{x}-\hat{y}$	$\hat{x}+\hat{z}$	$\hat{x}-\hat{z}$	$\hat{y}+\hat{z}$	$\hat{y}-\hat{z}$
Angle	π	$3\pi/2$	π	π	π	π	π	π
j'^{rot}	0.03333	0.03333	0.03333	0.03333	2.64575	0.57485	0.03333	0.03333
j_1^{rot}	2.00000	3.00000	0.50509	0.50509	1.00000	2.53276	1.71541	1.71541
j_2^{rot}	0.45510	0.67658	4.57172	4.57172		0.03333	0.13012	0.13012
j_3^{rot}	2.00000	3.00000	0.50509	0.50509		2.53276	1.71541	1.71541
j_4^{rot}								
j_5^{rot}								
t_1^{rot}	0.50027	0.42475	1.91411	0.89008	1.11072	0.57686	0.51303	1.06916
t_2^{rot}	2.13931	2.29036	0.33565	0.33565		1.56992	1.55767	1.55767
t_3^{rot}	0.50027	0.42475	0.89008	1.91411		0.57686	1.06916	0.51303
t_4^{rot}								
t_5^{rot}								
j_1	14.8320	6.08606	12.9511	2.98902	9.36914	5.01120	6.21125	5.20786
j_2	0.08568	0.07273	0.17844	0.32786	0.04832	0.06079	0.14018	0.06111
j_3	17.4859	5.41369	1.75872	10.2626	8.17962	8.18877	6.64681	5.73146
j_4	0.04172	0.15263	0.13529	0.10200	0.31474	0.04798	0.06600	0.09549
j_5	10.6823	11.8655	2.87996	12.5734	8.40274	4.43495	6.24976	4.24419
j_6	0.14942	0.09036	0.06331	0.06508	0.13463	0.10140	0.06618	0.10577
j_7	18.4109	7.12383	11.4745	11.8260	4.71318	8.08935	8.75777	5.42467
j_8	0.22390	0.33033	0.29352	0.22181	0.24977	0.27460	0.12328	0.09174
j_9	19.9055	6.73884	7.19879	10.0370	9.68484	1.04517	7.22767	3.56681
j_{10}	0.22414	0.06294	0.10262	0.05338	0.28410	0.10052	0.07137	0.06428
j_{11}	13.7704	10.7659	3.49491	14.3384	6.16179	7.94141	6.30792	8.25962
j_{12}	0.23365	0.31156	0.05490	0.24371	0.49621	0.09732	0.19631	0.18793
j_{13}	21.2667	8.21772	12.9055	2.82533	7.59476	5.90722	8.13722	2.81933
j_{14}	0.18113	0.05662	0.21813	0.08250	0.07428	0.22768	0.08147	0.06690
j_{15}	10.3561	5.26986	3.93531	12.2900	14.9265	2.69925	4.29169	4.53299
j_{16}	0.08696	0.10441	0.07098	0.07438	0.04470	0.06062	0.08320	0.08701
j_{17}	6.22164	5.54215	16.6152	9.95958	13.3491	5.46497	3.83547	6.02802
j_{18}	0.20041	0.11415	0.21540	0.27869	0.04341	0.27100	0.15614	0.33781
ϕ_1	1.75669	0.49652	3.09290	3.85330	3.10342	4.02203	5.43418	0.98434
ϕ_2	2.33422	3.96681	4.50049	1.47780	3.95197	4.57343	2.59242	4.13376
ϕ_3	5.30954	2.49781	2.81283	4.59337	0.93831	2.09934	3.69553	2.48926
ϕ_4	3.12939	2.27810	3.59551	1.79992	2.66582	3.83942	3.39603	2.08419
ϕ_5	3.28294	4.08082	5.27644	3.92107	4.21612	3.34398	1.55155	4.53314
ϕ_6	2.98278	3.30503	2.87973	2.89507	2.69878	3.40785	3.35411	3.41282
ϕ_7	2.97049	2.86190	3.01380	3.17126	4.52586	2.99563	0.90107	1.87910
ϕ_8	3.59125	3.44407	1.64479	3.88246	2.98595	2.30693	4.03589	4.29502
ϕ_9	1.48541	3.47186	5.16677	2.82468	3.74931	2.66493	1.96720	2.63959
ϕ_{10}	3.27256	2.84195	3.83777	3.36406	3.60174	5.02774	2.53451	3.23638
ϕ_{11}	5.26209	5.76930	2.23586	4.49378	0.60704	2.67576	5.92522	4.83535
ϕ_{12}	3.40959	2.13972	3.66723	2.42232	3.33144	2.96314	2.81749	1.66024
ϕ_{13}	3.45772	4.43079	0.72011	1.64091	2.42357	2.97994	4.50915	4.35308
ϕ_{14}	2.92306	2.96829	4.41970	3.49835	3.12093	2.89307	3.28735	3.44457
ϕ_{15}	3.57310	3.28504	3.75495	2.01767	4.37853	3.39137	2.10098	2.08324
ϕ_{16}	3.08844	2.50621	3.16872	3.79660	3.71673	3.13385	3.66449	2.83612
ϕ_{17}	2.42464	3.66783	4.04567	2.14381	1.88580	0.77083	2.15351	3.94458
ϕ_{18}	3.14159	3.14159	3.14159	3.14159	3.14159	3.14159	3.14159	3.14159

TABLE VI. Parameters for the dynamically corrected $\hat{x} \pm \hat{y} \pm \hat{z}$ rotations for a model with constant J_i.

Axis Angle	$\hat{x}+\hat{y}+\hat{z}$ $2\pi/3$	$\hat{x}+\hat{y}+\hat{z}$ $4\pi/3$	$-\hat{x}+\hat{y}+\hat{z}$ $2\pi/3$	$-\hat{x}+\hat{y}+\hat{z}$ $4\pi/3$	$\hat{x}-\hat{y}+\hat{z}$ $2\pi/3$	$\hat{x}-\hat{y}+\hat{z}$ $4\pi/3$	$\hat{x}+\hat{y}-\hat{z}$ $2\pi/3$	$\hat{x}+\hat{y}-\hat{z}$ $4\pi/3$
j'^{rot}	0.03333	0.03333	0.03333	0.03333	0.03333	0.03333	0.03333	0.03333
j_1^{rot}	0.56170	0.74456	0.32145	0.29210	0.56170	0.74456	0.29210	0.32145
j_2^{rot}	2.41400	3.22657	14.0228	8.36716	2.41400	3.22657	8.36716	14.0228
j_3^{rot}	0.56170	0.74456	0.32145	0.29210	0.56170	0.74456	0.29210	0.32145
j_4^{rot}								
j_5^{rot}								
t_1^{rot}	2.21343	1.97092	1.17574	1.18212	0.52564	0.54891	1.83346	1.81513
t_2^{rot}	0.40078	0.62001	0.14898	0.12427	0.40078	0.62001	0.12427	0.14898
t_3^{rot}	0.52564	0.54891	1.81513	1.83346	2.21343	1.97092	1.18212	1.17574
t_4^{rot}								
t_5^{rot}								
j_1	10.7661	11.5740	5.00930	5.44077	10.2269	18.7776	5.90484	7.15782
j_2	0.11510	0.28828	0.09538	0.29018	0.11723	0.05318	0.31409	0.17930
j_3	8.89117	3.65918	19.1213	11.3119	10.2021	10.0969	4.31741	7.46876
j_4	0.20559	0.05901	0.09606	0.04124	0.09354	0.15789	0.06110	0.05518
j_5	4.83475	25.6828	16.7694	9.32045	8.16447	22.2191	6.51526	5.27719
j_6	0.13395	0.06718	0.05482	0.43300	0.11700	0.17654	0.08278	0.05364
j_7	4.48507	3.05551	5.41672	17.3620	11.0271	3.90888	6.85651	17.3085
j_8	0.04527	0.04005	0.26657	0.17560	0.21473	0.32907	0.18002	0.07704
j_9	2.18431	6.29185	4.22555	3.67047	12.0647	21.4374	0.55896	13.0452
j_{10}	0.04490	0.20990	0.50948	0.50657	0.07343	0.39065	0.86102	0.13407
j_{11}	17.2965	5.91075	18.5654	18.3140	8.36832	20.4086	7.40366	15.0703
j_{12}	0.04339	0.06178	0.03382	0.11821	0.27946	0.04014	0.13026	0.05362
j_{13}	6.82614	27.2096	19.6292	6.85666	6.94247	26.3145	7.57882	6.28250
j_{14}	0.14376	0.06382	0.34693	0.30954	0.16238	0.16546	0.10877	0.19997
j_{15}	5.06561	4.64735	4.87618	15.9969	7.65720	9.27366	4.90249	5.97533
j_{16}	0.22779	0.05061	0.03903	0.04383	0.07173	0.13057	0.06292	0.05197
j_{17}	7.64291	5.61436	26.8249	12.2456	6.38671	20.9800	6.40504	6.57259
j_{18}	0.29524	0.36538	0.51048	0.70207	0.22653	0.26497	0.46266	0.07298
ϕ_1	1.86227	2.26580	1.99571	2.43151	3.12683	3.13524	2.02942	4.30594
ϕ_2	2.39636	1.49241	3.47874	2.99874	3.84944	3.11065	3.65426	3.40109
ϕ_3	3.09316	3.37813	2.91187	3.89836	1.93029	3.27606	3.38573	2.83522
ϕ_4	4.08038	3.08759	2.24376	3.35420	2.90934	3.18770	3.04261	3.13690
ϕ_5	1.96027	3.05081	5.45630	4.98881	4.25714	1.86445	3.74543	2.14373
ϕ_6	3.21424	3.14847	4.07229	2.53448	3.14612	2.39157	2.14569	2.56715
ϕ_7	4.16769	3.99172	2.41585	2.77336	4.61272	4.62757	4.16869	4.07547
ϕ_8	2.17830	3.35751	2.70266	3.66705	2.39626	3.51918	2.41949	3.83791
ϕ_9	3.57785	5.37022	3.51253	1.23518	4.24717	1.58182	4.95506	2.07100
ϕ_{10}	2.70602	1.22627	1.69335	3.06442	3.74150	4.54924	1.50139	2.59654
ϕ_{11}	1.35997	5.20760	3.18859	2.74756	0.31262	2.40164	2.38693	5.09851
ϕ_{12}	4.48065	2.96135	2.94189	3.71204	3.34590	3.69582	4.17284	3.64342
ϕ_{13}	2.31352	2.31340	4.59434	2.49796	1.86224	1.83430	2.89132	4.21655
ϕ_{14}	3.43885	2.63958	3.43121	3.79832	2.96260	3.20157	3.45387	2.74168
ϕ_{15}	3.35857	2.41218	2.67771	2.05334	3.99016	2.92032	2.11405	2.92801
ϕ_{16}	3.31546	3.96840	2.93719	2.76419	2.94494	2.73833	3.89997	3.22086
ϕ_{17}	2.51257	4.36821	2.44037	6.09444	3.72074	6.00654	1.43218	3.49669
ϕ_{18}	3.14159	3.14159	3.14159	3.14159	3.14159	3.14159	3.14159	3.14159

[1] A. G. Fowler, M. Mariantoni, J. M. Martinis, and A. N. Cleland, Phys. Rev. A **86**, 032324 (2012).

[2] D. Loss and D. P. DiVincenzo, Phys. Rev. A **57**, 120 (1998).

[3] K. Nowack, M. Shaffei, M. Laforest, G. E. D. K. Prawiroatmodjo, L. R. Schreiber, C. Reichl, W. Wegscheider, and L. M. K. Vandersypen, Science **333**, 1269 (2011).

[4] J. J. Pla, K. Y. Tan, J. P. Dehollain, W. H. Lim, J. J. L. Morton, D. N. Jamieson, A. S. Dzurak, and A. Morello, Nature (London) **489**, 541 (2012).

[5] J. J. Pla, K. Y. Tan, J. P. Dehollain, W. H. Lim, J. J. L. Morton, F. A. Zwanenburg, D. N. Jamieson, A. S. Dzurak, and A. Morello, Nature (London) **496**, 334 (2013).

[6] M. Veldhorst, J. C. C. Hwang, C. H. Yang, A. W. Leenstra, B. de Ronde, J. P. Dehollain, J. T. Muhonen, F. E. Hudson, K. M. Itoh, A. Morello, and A. S. Dzurak, Nat. Nanotechnol. **9**, 981 (2014).

[7] F. R. Braakman, P. Barthelemy, C. Reichl, W. Wegscheider, and L. M. K. Vandersypen, Nat. Nanotechnol. **8**, 432 (2013).

[8] T. Otsuka, T. Nakajima, M. R. Delbecq, S. Amaha, J. Yoneda, K. Takeda, G. Allison, T. Ito, R. Sugawara, A. Noiri *et al.*, Sci. Rep. **6**, 31820 (2016).

[9] T. Ito, T. Otsuka, S. Amaha, M. R. Delbecq, T. Nakajima, J. Yoneda, K. Takeda, G. Allison, A. Noiri, K. Kawasaki, and S. Tarucha, Sci. Rep. **6**, 39113 (2016).

[10] J. Levy, Phys. Rev. Lett. **89**, 147902 (2002).

[11] J. Petta, A. Johnson, J. Taylor, E. Laird, A. Yacoby, M. Lukin, C. Marcus, M. Hanson, and A. Gossard, Science **309**, 2180 (2005).

[12] S. Foletti, H. Bluhm, D. Mahalu, V. Umansky, and A. Yacoby, Nat. Phys. **5**, 903 (2009).

[13] I. van Weperen, B. D. Armstrong, E. A. Laird, J. Medford, C. M. Marcus, M. P. Hanson, and A. C. Gossard, Phys. Rev. Lett. **107**, 030506 (2011).

[14] B. M. Maune, M. G. Borselli, B. Huang, T. D. Ladd, P. W. Deelman, K. S. Holabird, A. A. Kiselev, I. Alvarado-Rodriguez, R. S. Ross, A. E. Schmitz *et al.*, Nature (London) **481**, 344 (2012).

[15] M. D. Shulman, O. E. Dial, S. P. Harvey, H. Bluhm, V. Umansky, and A. Yacoby, Science **336**, 202 (2012).

[16] O. E. Dial, M. D. Shulman, S. P. Harvey, H. Bluhm, V. Umansky, and A. Yacoby, Phys. Rev. Lett. **110**, 146804 (2013).

[17] M. D. Shulman, S. P. Harvey, J. M. Nichol, S. D. Bartlett, A. C. Doherty, V. Umansky, and A. Yacoby, Nat. Commun. **5**, 5156 (2014).

[18] M. D. Reed, B. M. Maune, R. W. Andrews, M. G. Borselli, K. Eng, M. P. Jura, A. A. Kiselev, T. D. Ladd, S. T. Merkel, I. Milosavljevic *et al.*, Phys. Rev. Lett. **116**, 110402 (2016).

[19] F. Martins, F. K. Malinowski, P. D. Nissen, E. Barnes, S. Fallahi, G. C. Gardner, M. J. Manfra, C. M. Marcus, and F. Kuemmeth, Phys. Rev. Lett. **116**, 116801 (2016).

[20] D. P. DiVincenzo, D. Bacon, J. Kempe, G. Burkard, and K. B. Whaley, Nature (London) **408**, 339 (2000).

[21] J. Medford, J. Beil, J. M. Taylor, S. D. Bartlett, A. C. Doherty, E. I. Rashba, D. P. DiVincenzo, H. Lu, A. C. Gossard, and C. M. Marcus, Nat. Nanotechnol. **8**, 654 (2013).

[22] J. Medford, J. Beil, J. M. Taylor, E. I. Rashba, H. Lu, A. C. Gossard, and C. M. Marcus, Phys. Rev. Lett. **111**, 050501 (2013).

[23] K. Eng, T. D. Ladd, A. Smith, M. G. Borselli, A. A. Kiselev, B. H. Fong, K. S. Holabird, T. M. Hazard, B. Huang, P. W. Deelman *et al.*, Sci. Adv. **1**, e1500214 (2015).

[24] Y.-P. Shim and C. Tahan, Phys. Rev. B **93**, 121410(R) (2016).

[25] Z. Shi, C. B. Simmons, J. R. Prance, J. K. Gamble, T. S. Koh, Y.-P. Shim, X. Hu, D. E. Savage, M. G. Lagally, M. A. Eriksson, M. Friesen, and S. N. Coppersmith, Phys. Rev. Lett. **108**, 140503 (2012).

[26] D. Kim, Z. Shi, C. B. Simmons, D. R. Ward, J. R. Prance, T. S. Koh, J. K. Gamble, D. E. Savage, M. G. Lagally, M. Friesen *et al.*, Nature (London) **511**, 70 (2014).

[27] D. Kim, D. R. Ward, C. B. Simmons, D. E. Savage, M. G. Lagally, M. Friesen, S. N. Coppersmith, and M. A. Eriksson, npj Quant. Inf. **1**, 15004 (2015).

[28] J. M. Nichol, L. A. Orona, S. P. Harvey, S. Fallahi, G. C. Gardner, M. J. Manfra, and A. Yacoby, npj Quant. Inf. **3**, 3 (2017).

[29] H. Bluhm, S. Foletti, D. Mahalu, V. Umansky, and A. Yacoby, Phys. Rev. Lett. **105**, 216803 (2010).

[30] H. Bluhm, S. Foletti, I. Neder, M. Rudner, D. Mahalu, V. Umansky, and A. Yacoby, Nat. Phys. **7**, 109 (2011).

[31] A. Sergeevich, A. Chandran, J. Combes, S. D. Bartlett, and H. M. Wiseman, Phys. Rev. A **84**, 052315 (2011).

[32] J. T. Muhonen, J. P. Dehollain, A. Laucht, F. E. Hudson, T. Sekiguchi, K. M. Itoh, D. N. Jamieson, J. C. McCallum, A. S. Dzurak, and A. Morello, Nat. Nanotechnol. **9**, 986 (2014).

[33] F. K. Malinowski, F. Martins, P. D. Nissen, E. Barnes, Ł. Cywiński, M. S. Rudner, S. Fallahi, G. C. Gardner, M. J. Manfra, C. M. Marcus, and F. Kuemmeth, Nat. Nanotechnol. **12**, 16 (2017).

[34] W. M. Witzel and S. D. Sarma, Phys. Rev. Lett. **98**, 077601 (2007).

[35] W. M. Witzel and S. D. Sarma, Phys. Rev. B **76**, 241303 (2007).

[36] B. Lee, W. M. Witzel, and S. D. Sarma, Phys. Rev. Lett. **100**, 160505 (2008).

[37] N. Yokoshi, H. Imamura, and H. Kosaka, Phys. Rev. B **81**, 161305 (2010).

[38] A. V. Nenashev, A. F. Zinovieva, A. V. Dvurechenskii, A. Yu. Gornov, and T. S. Zarodnyuk, J. Appl. Phys. **117**, 113905 (2015).

[39] J. C. C. Hwang, C. H. Yang, M. Veldhorst, N. Hendrickx, M. A. Fogarty, W. Huang, F. E. Hudson, A. Morello, and A. S. Dzurak, Phys. Rev. B **96**, 045302 (2017).

[40] X. Hu and S. D. Sarma, Phys. Rev. A **64**, 042312 (2001).

[41] E. Nielsen, E. Barnes, J. P. Kestner, S. D. Sarma, Phys. Rev. B **88**, 195131 (2013).

[42] F. Martins, F. K. Malinowski, P. D. Nissen, S. Fallahi, G. C. Gardner, M. J. Manfra, C. M. Marcus, and F. Kuemmeth, Phys. Rev. Lett. **119**, 227701 (2017).

[43] X. Wang, L. S. Bishop, J. P. Kestner, E. Barnes, K. Sun, and S. D. Sarma, Nat. Commun. **3**, 997 (2012).

[44] X. Wang, L. S. Bishop, E. Barnes, J. P. Kestner, and S. D. Sarma, Phys. Rev. A **89**, 022310 (2014).

[45] R. E. Throckmorton, C. Zhang, X.-C. Yang, X. Wang, E. Barnes, and S. D. Sarma, Phys. Rev. B **96**, 195424 (2017).

[46] J. Zeng, X.-H. Deng, A. Russo, and E. Barnes, arXiv:1703.00816v2.

[47] S. D. Sarma, R. E. Throckmorton, and Y.-L. Wu, Phys. Rev. B **94**, 045435 (2016).

[48] Y.-L. Wu and S. D. Sarma, Phys. Rev. B **96**, 165301 (2017).
[49] X. Wang, E. Barnes, and S. D. Sarma, npj Quant. Inf. **1**, 15003 (2015).
[50] R. Li, X. Hu, and J. Q. You, Phys. Rev. B **86**, 205306 (2012).
[51] J. P. Kestner, X. Wang, L. S. Bishop, E. Barnes, and S. D. Sarma, Phys. Rev. Lett. **110**, 140502 (2013).
[52] E. Barnes (private communication).
[53] J. Medford, Ł. Cywiński, C. Barthel, C. M. Marcus, M. P. Hanson, and A. C. Gossard, Phys. Rev. Lett. **108**, 086802 (2012).